Submitted: 18/08/15
Accepted: 10/03/16

Research Article

[1]Department of Physics, McGill University, Montreal, QC, Canada

Email Correspondence

ling.lin2@mail.mcgill.ca

Alistair Barton[1], Ling Lin[1], Shoma Yamanouchi[1]

Cosmic Strings and The Origins of Globular Clusters

Abstract

Background: Globular clusters are galactic structures whose origin is not well understood. In this paper we propose that their origin may be found in the accretions formed around cosmic string loops.

Methods: To test this hypothesis we derived the mass distribution that would be associated with the accretions and compared it to the observed mass distribution of globular clusters in our galaxy. Our derived distribution left us one free parameter (cosmic string tension) which we varied to optimize the fit. Once optimized, we compared the shape of the distribution and the number density that our model predicted with empirical observations. Later, we derived how velocity effects would alter the shape of this distribution.

Results: We achieved significant agreement between our model and observed values. Furthermore, the optimal tension corresponds to particle physics theories that have not been ruled out. Our analysis further suggests that globular clusters form around slowly moving (< 3% the speed of light) cosmic string loops; any model with significantly faster cosmic string loops would contradict our hypothesis.

Limitations: Our results were obtained by using numerous approximations (such as the Zel'dovich approximation) and thus should be treated as an order of magnitude estimation. Our data was also limited to observed globular clusters within the Milky Way, limiting our sample size to approximately 120 globular clusters.

Conclusions: We managed to obtain strong agreement between our model and observed globular clusters, suggesting that they may be seeded by cosmic string loops. This also serves to explain many other characteristics of globular clusters, such as age, density and location. The analyses used in this report can also be used when considering the formation of other accretion objects, such as ultra-compact-minihalos.

Background

Inflationary Cosmology

The main focus of cosmology is the study of the Universe on the largest of scales. In the inflationary model, the Universe expanded exponentially after the Big Bang. This exponential growth era is known as the inflationary epoch, and lasted from 10^{-36} seconds to 10^{-32} seconds after the Big Bang, after which the Universe continued to grow, but at a less accelerated rate. It is important to note that "growth" here signifies a stretching of space in all directions at all points.

Following inflation were the successive radiation-dominated and matter-dominated eras. The transition time between the two, or the time of equal matter and radiation, is denoted t_{eq}. Fig. 1 shows the timeline of the Universe, and how it evolved over time. Before t_{eq}, much of the energy in the Universe was in the form of radiation, dominating the Universe in a state of disorder and preventing electrons from being captured by nuclei. It is only after t_{eq} that we begin to see the formation of neutral hydrogen and large structures such as stars and galaxies (this occurs slightly after t_{eq}: the time of Cosmic Microwave Radiation). It is in explaining the formation of these stellar objects that cosmic strings come into play.

Cosmic String Loops

The early Universe is known to have been nearly uniform in all aspects. This raises the question of how the mass discrepancies in today's Universe arose (e.g., the difference in stellar density within and outside of galaxies). The inflationary model partially solves this problem by allowing random early Universe quantum fluctuations to grow to a large scale and have a

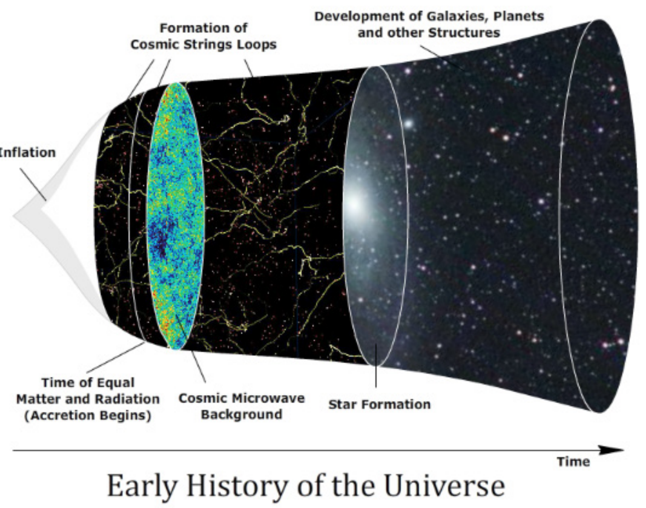

Fig. 1. Artistic impression of the early history of the Universe with reference to (1, 2) by Ling Lin. Note that cosmic string loops form during both the radiation and matter dominated epochs (to the left and right of the time of equal matter and radiation respectively), while structure formation occurs much later.

significant role in the evolution of our Universe. However, it is not successful at explaining the origin of globular clusters, so we turn to cosmic string loops as a potential source.

In the early Universe, all of space was highly dense and energetic (a "cosmic soup"). This corresponds to an excited state in each of the elementary-particle-fields. It is imperative to note that these excitations were statistically homogenous throughout the field. However, as the Universe cooled down, the excitations in the field died down. During this cooling period, topological defects in the fields may have formed. These defects arise in cases where the field values minimizing the potential energy form a circle in field space around a region of higher energy (we will call it a 'hole'). Thus, as the excitations cool, the field values at different points in space take on values, bordering the hole, corresponding to the minimum potential (this is referred to as *symmetry breaking*). However, due to causality (no information can travel faster than the speed of light), there can be no correlation between the field values of distant enough regions of space. This causes the field values along some closed paths to take the minimum values encircling the hole in field space, requiring a location in the interior of the path where there must be, to retain continuity of the field, a core where the potential energy is not at its minimum value, causing a defect of extremely high energy density. For certain potentials (arising in a large class of particle physics models beyond the Standard Model of particle physics), these defects are cosmic strings: one-dimensional regions of extremely high energy density. Because these strings form early in the Universe (before t_{eq}), they would have ample time to attract enough matter to form large scale objects such as galaxies (see Fig. 1).

Cosmic strings may be seen as analogous to defect lines in crystals and vortex lines in superfluids and conductors. These strings may also intersect each other and form closed loops (Fig. 2). These loops could also play a role in structure formation, and would start to accrete matter at t_{eq}: when matter becomes the dominant form of energy.

Introduction

Globular clusters are very tightly bound spherical collections of high star population. They are unique for being found in galactic halos, rather than in the galactic disks, and being much older than other star clusters. Their origin is not yet well understood. (3, 4)

In this paper, we propose that globular clusters may have their origin in the activity of cosmic string loops: onedimensional objects of trapped energy arising from symmetry breaking in certain particle physics models. These models will result in a network of cosmic strings of infinite length in the early Universe that will persist until the present day.

The network of cosmological strings is characterized by a mean separation distance $\zeta(t)$ that scales with the expansion of the Universe. This separation distance determines the likelihood of the collision of cosmic strings, which produces loops. Likewise, the resulting network of cosmic string loops, which we will focus on, is characterized by a critical loop radius $R_{cl}(t)$ whose corresponding mass dominates the mass distribution of loops.

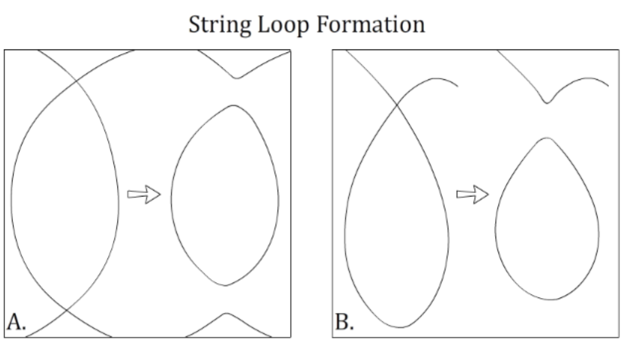

Fig. 2. Here we can see loop formation by two different mechanisms: intersection of two string segments on the left (resulting in a loop in addition to the two original string segments), and self-intersection of a segment on the right (resulting in a loop in addition to the original string segment).

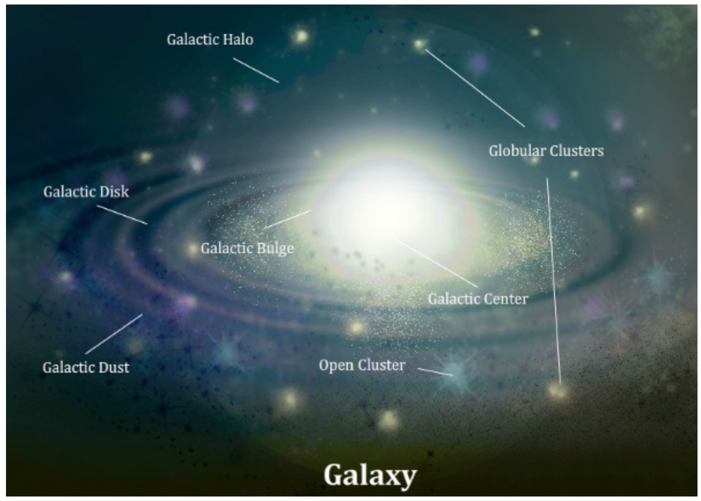

Fig. 3. Artistic impression of the Milky Way Galaxy by Ling Lin.

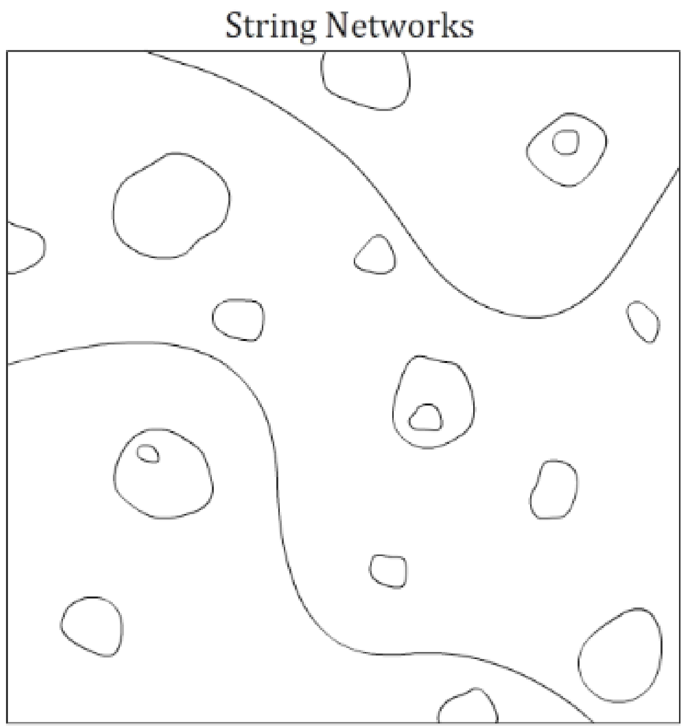

Fig. 4. A network of strings. We can see two infinite strings in addition to numerous loops of various radii.

These loops are present at very early times, forming non-linear objects before the formation of galaxies. The objects could then evolve into dense clumps which would be distributed through the galactic halo (as string loops would initially be roughly uniformly distributed in the region that falls in to form the galaxy).

Meanwhile, the cosmological effect of the cosmic strings is characterized by the constant mass per unit length of the strings μ (usually expressed as the dimensionless $G\mu$, where G is the gravitational constant).

In this study, we fix $G\mu$ by demanding that the mass accreting around a loop with radius R_{cl} agree with the observed peak in the globular cluster mass distribution. From fixing $G\mu$, we are then able to predict both the number density and mass distribution of globular clusters and find that they agree with the observed results. As accretion around loops starts shortly after creation—at the time of matter and radiation equality—this mechanism offers an explanation for why globular clusters are the oldest structures in a galaxy. Our proposed mechanism further offers an explanation for why globular clusters are found in the galactic halo, as previously described.

In the following sections, we will first review the relevant literature on cosmic string loop distributions. Then, we will present our computations of $G\mu$ and the resulting predictions it makes about globular clusters, comparing with observed values. We analyze how incorporating the initial velocity of loops affects our predicted mass distribution of globular clusters. This is then once more compared with the observed mass distribution of globular clusters in our Milky Way galaxy. Finally, we present our conclusions.

Cosmic String Loop Distribution

We can characterize cosmic strings by their tension (or mass per unit length) μ which is related to the energy scale η of the new physics by $\mu = \eta^2$. It is important to note that μ is proportional to the gravitational strength generated by the string.

Cosmic strings have historically been hypothesized (5) to have seeded various cosmic structures. The 'one string–one galaxy' hypothesis—that galaxies originated by coalescing around cosmic strings—required a string tension of $G\mu \sim 10^{-6}$, corresponding to an energy scale beyond observed physics. However this model has since been ruled out by observations of the Cosmic Microwave Background (CMB) radiation (6, 7, 8, 9, 10, 11, 12, 13, 14) which set an upper limit on the string tension of

$$G\mu < 2\,(10^{-7}) \quad [1]$$

This is a generous bound which may be lowered by further analyzing CMB maps (15, 16, 17) or by constraints on the gravitational waves generated by strings. (18) These constraints restrict string loops from being heavy enough to produce large scale structures, however, strings can still play a significant role in cosmology while observing this bound, as we will explore.

In this paper, we will consider a model for the distribution of strings which implies that the loop's radius R (which remains approximately constant) is proportional to its time of formation t_f (19, 20) Once formed, the number density of loops of radius R will decrease due to the expansion of space, and existing loops will slowly decay as they lose energy to gravitational radiation. (21) This leads to loops with a radius less than a certain critical radius $R_{c1}(t)$ decaying within the age of the Universe.

From what we know, we can determine the number density, $n(R,t)$, of string loops of radius R for times after matter-radiation equality, to depend on whether loops were formed before or after t_{eq}. (22) We can simplify this by ignoring loops forming at a time ti after t_{eq} (as they would have less times to accrete matter), giving us the number density seen in Fig. 5. We can then find the total number density of strings by integrating $n(R,t)$ over R. It is important to note that the number density will reach its peak at $R \leq R_{c1}(t)$, and its peak will be proportional to $(G\mu)^{-5/2}$. (22) We also can see that smaller values of $G\mu$ will lead to larger loop number densities, allowing more to fall into galaxies during galaxy formation.

Using the results we've obtained from this section, we are now prepared to examine the possibility that string loops seed the globular clusters situated in the galactic halo.

Globular Clusters from Cosmic Strings

Linear cosmological perturbation theory tells us that accretion of matter around a cosmic string loop starts at t_{eq}. At this time, the mass distribution of the string loops is dominated by the mass M_c associated with loops of the critical radius R_{c1}. Though these cosmic string loops will have decayed by the present time, the objects they seed will continue to grow.

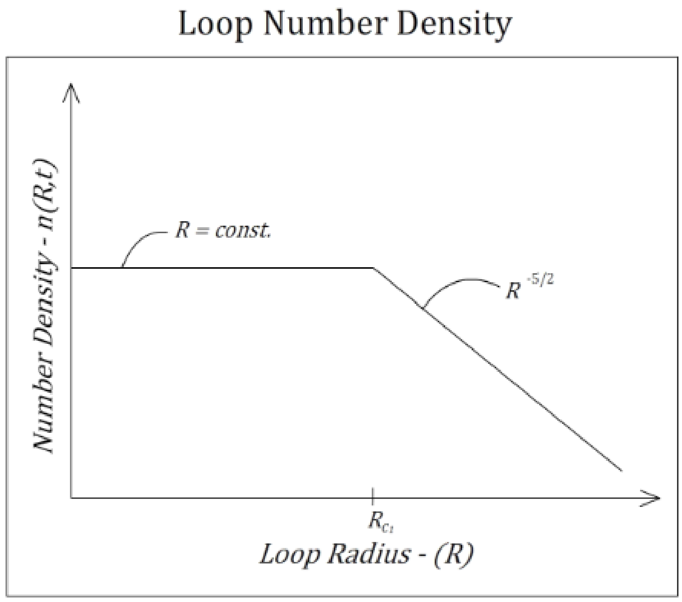

Fig. 5. The distribution of cosmic string loop radii. Note that there is a large drop-off after R_{c1}.

Assuming accretion continues to the present time, the mass which has accreted about these seed loops will have a dependence on $G\mu$. (23) Taking the peak mass of globular clusters in our galaxy to be $M_{GC} \sim 10^5$ solar masses into the number density formula, we obtain

$$G\mu \sim 10^{-9.5} \approx 3(10^{-10}) \quad [2]$$

We estimate the number density of globular clusters within a galaxy by integrating the number density in Fig. 5 over all radius values R, and including a factor to compensate for the collapsing of loops around the galaxy into the galaxy. (24) Inserting our estimate for $G\mu$ from Equation [2], we get a number density of globular clusters within galaxies of: (22)

$$n_{local} \sim 10^{-2}\,(kpc)^{-3} \quad [3]$$

Note that this is of the same order of magnitude as the observed number density of globular clusters inside the Milky Way.

In our analysis so far, we have taken only the peak mass of our string mass distribution M_c to fix our only free parameter: the string tension. We now derive the rest of the mass distribution. As loops with radius $R > R_{c1}$ barely decay over the time scale of the Universe, we can say that for $M > M_c$, the mass distribution will follow the radius distribution and scale as $M^{-5/2}$. For loops of smaller radius (and $M < M_c$) that do decay, we predict a linear decay since the loop radius distribution is constant; however, loops with radius smaller than R_{c1} live only a fraction of the age of the Universe.

In Fig. 6, we compare the predicted distribution (the solid lines) and the observed distribution (25) (histogram values) of globular clusters in the Milky Way. The curves are obtained by making a change of variable from R to M on the number density of loops when accretion starts at t_{eq} $(n(R,t_{eq}) \rightarrow n(M,t_{eq})\,(dR/dM))$, and then accounting for the expansion of space and the accretion of matter (using cosmological red-shift and the Zel'dovich approximation), (24) finally we multiply by the bin size and the volume of the Milky Way. We also plot various values of $G\mu$ and see that increasing $G\mu$ increases the peak mass but decreases the predicted number of globular clusters. The solid blue curves minimizes χ^2 and is a surprisingly good fit of both the shape and the peak number density at the same value of $G\mu$ at $G\mu = 5.43(10^{-10})$. The shape and the order of magnitude accuracy in particular are reassuring, as the scale of the function depends on a few approximations and values obtained from simulation results, and therefore has some wiggle room while the shape of the function is precisely derived.

A notable omission in this section is that we have neglected the interactions between globular clusters and the highly chaotic processes of galaxy

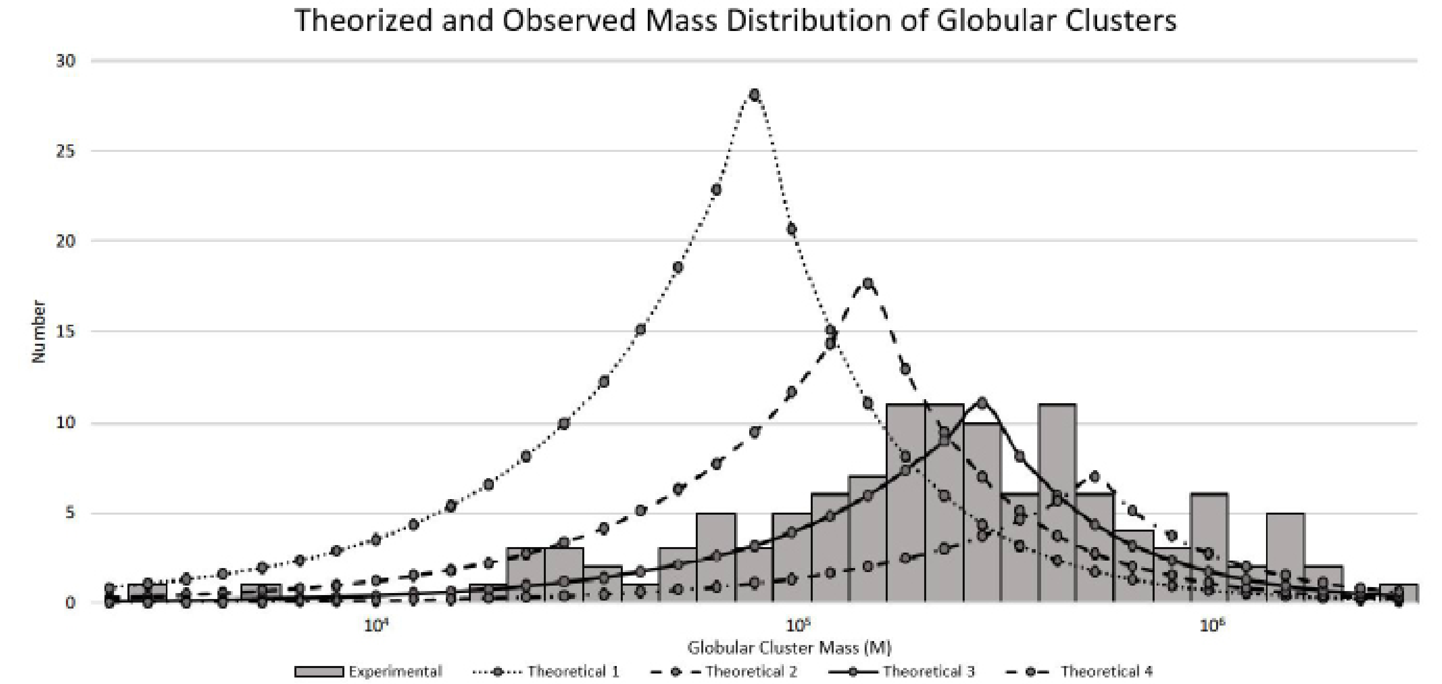

Fig. 6. Our model's predicted globular cluster mass distributions in the Milky Way for various values of Gμ. The horizontal axis is mass on a logarithmic scale, the vertical axis gives the expected number of clusters on a linear scale. The histogram show the data taken from (25). For the curves Theoretical 1, 2, 3, 4 we set Gμ as $2.92(10^{-10})$, $3.98(10^{-10})$, $5.43(10^{-10})$ and $7.41(10^{-10})$ respectively. Curve 3 ($G\mu = 5.43(10^{-10})$) minimizes χ^2.

formation that may cause changes to the mass function as a function of time in our analysis.

Effect of Cosmic String Velocity

All of the calculations above assumed that cosmic strings are created, and remain, at rest. Recent numerical simulations (26) tell us that loops are typically born with translational velocities that are sizable fractions of the speed of light. Since long string segments usually have relativistic speeds, it is unsuprising that string loops will also gain significant velocities as they split off from string segments. When velocities are taken into consideration, accretion will not be spherically symmetric. Additionally, accretion onto a moving loop may be much less efficient compared to accretion on a stationary loop. It should be noted, however, that loop velocities also slow down as they age due to the expansion of space (so called 'red-shifting'), dampening the effect. In this section, we will approach the effect velocities through two different analyses: one considering spherical accretions and one considering more irregular accretions.

Analysis 1

We first focus on loop velocities that give a tight spherical accretion by making sure the distance $\Delta r(R)$ the centre of the loop has moved before decaying is smaller than the current physical distance $h(R,t_0)$ (27) from the center of a string loop to the accreted mass shell (in such a way we can be sure the loop remains within the accretion region):

$$\Delta r(R) < h(R,t_0) \quad [4]$$

If the loop moves further than this, we assume that no globular clusters forms. Writing the displacement $\Delta r(R)$ in (Equation [4]) as the integral of velocity from t_{eq}, when strings loops begin accreting mass, to the present time, we obtain an upper bound v_i on the initial velocity of accreting loops. Approximating the distribution of initial velocities in each of three spatial directions to be a step function and taking the integral of the velocity distribution over accreting velocities (from zero to v_i), we find that the rate of globular cluster formation is suppressed by a multiplicative factor $S(R)$:

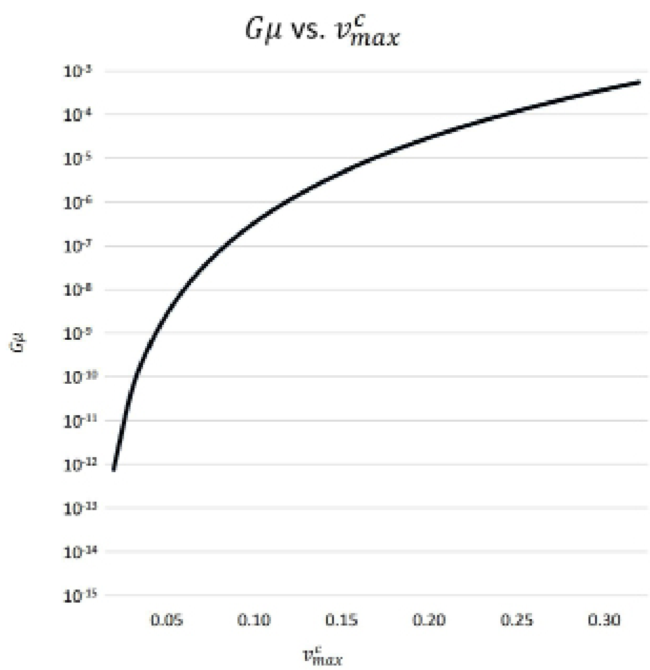

Fig. 7. Analysis 1 - Relation between Gμ and v^c_{max}. The horizontal axis is velocity on a linear scale and the vertical axis gives the Gμ on a logarithmic scale. Note that if, for a given Gμ, v_{max} (as determined by simulations) falls into the region below the curve then $R_{c1} > R_{c2}$; likewise, $R_{c1} < R_{c2}$ if v_{max} is in the region above the curve.

$$S(R) \text{ proportional to } (G\mu)R^{-1/2}v^{-3}_{max}, \quad [5]$$

where v_{max} is the maximum velocity of string loops, obtained through simulations. Note that this suppression factor only applies if it is less than 1. Thus, setting $R_{c2}(G\mu,v_{max})$ such that $S(R_{c2}) = 1$, we find that for values of $R < R_{c2}$, there is no suppression from velocity effects and for $R > R_{c2}$ the suppression is given by Equation [5]. It is important to note that R_{c2} is a decreasing function of v_{max}–unlike R_{c1}, which is independent of v_{max} (re-

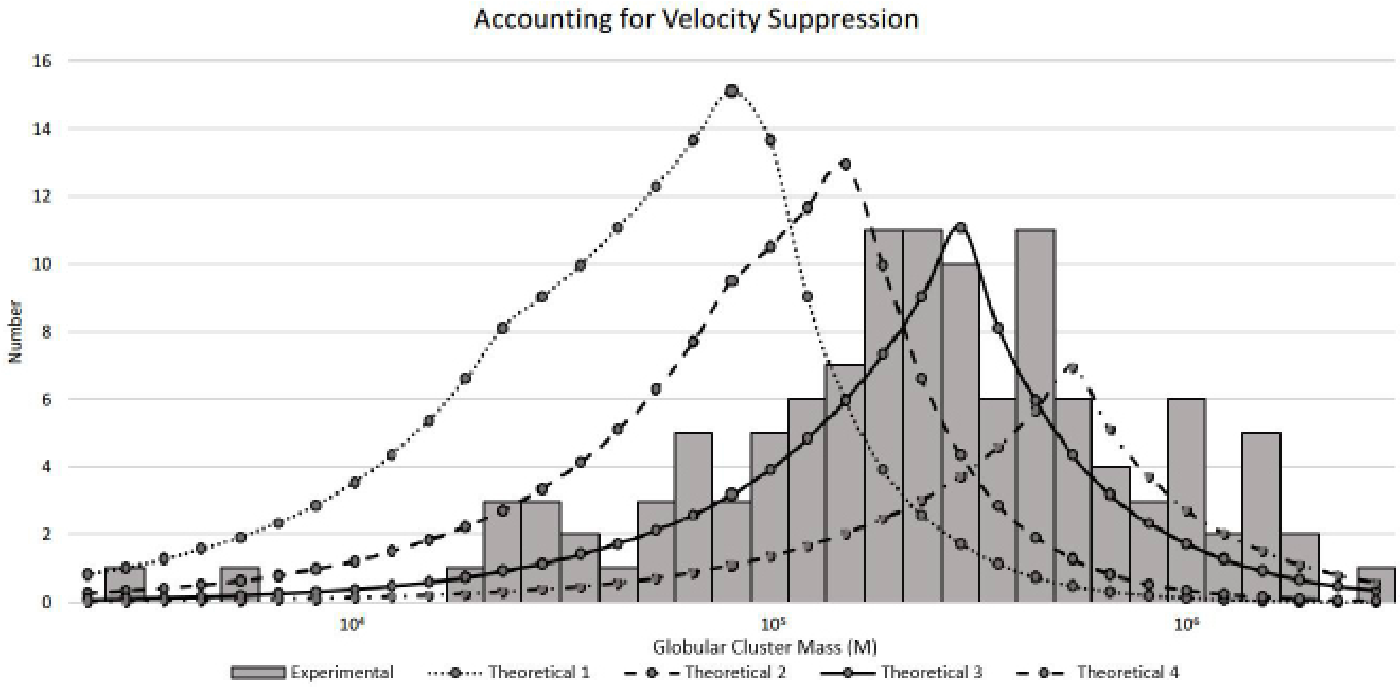

Fig. 8. Analysis 1 - Dependence of the mass function on Gμ at v_{max} =3 .00(10^{-2}). The horizontal axis is mass on a logarithmic scale, the vertical axis gives the number density on a linear scale. The histogram shows data taken from (25). For the curves Theoretical 1, 2, 3, 4 we set Gμ as 2.92(10^{-10}), 3 .98(10^{-10}), 5.43(10^{-10}), and 7 .41(10^{-10}), respectively. Noitce that for curves 1 and 2, $R_{c2} < R_{c1}$; for curve 3, $R_{c2} = R_{c1}$; and for the solid green curve $R_{c2} > R_{c1}$. Curve 3 minimizes χ^2 for this particular v_{max}.

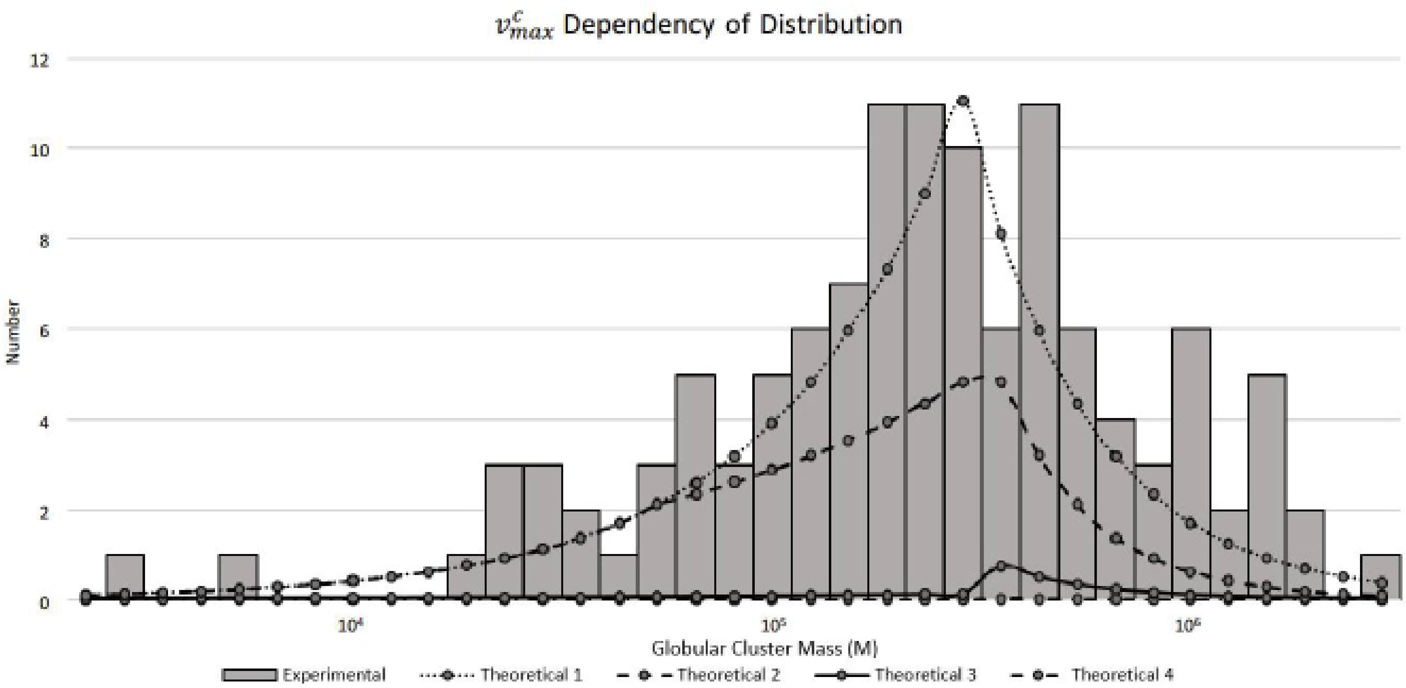

Fig. 9. Analysis 1 - Dependence of the mass function at Gμ = 5.43(10^{-10}) on v^{max}. For the curves Theoretical 1, 2, 3, 4 we set v_{max} as 1.00(10^{-1}), 6.46(10^{-2}), 3.44(10^{-2}) and 3.00(10-2) respectively. Notice that for all v_{max}< 3.00(10^{-2}) we would obtain curve 4. The axes and data are the same as in the previous figure.

call that R_{c1} is the peak of the mass distribution when we ignore velocity effects). We can then obtain a critical maximum velcocity v^c_{max} at which $R_{c2}(v^c_{max})=R_{c1}$:

$$v^c_{max} \textit{ proportional to } (G\mu)^{1/6} \quad [6]$$

Note that v^c_{max} is solely a function of $G\mu$, whose relation is graphed in Fig. 7. Hence, improving cosmic string loop simulations will deterimine if v^c_{max} is reliable and will give insight to the bounds on the string tension parameter. The importance of v^c_{max} is that it allows us to classify our models into two species. If we have v_{max} such that $R_{c2}(v_{max}) > R_{c1}(=R_{c2}(v^c_{max}))$, then v^c_{max} is an upper bound for v_{max}; likewise, for $R_{c2}(v_{max}) < R_{c1}$, we will have $v_{max} > v^c_{max}$. This is illustrated in Fig. 7. Inputting the suppression factor into our earlier calculations, we obtain an updated relation between $G\mu$ and the distribution in Fig. 8 and a new dependence on v_{max} in Fig. 9. In the case where $R_{c2} > R_{c1}$, the mass distribution scales as M^{-3} for $R > R_{c2}$, as $M^{-5/2}$ for $R_{c2} > R > R_{c1}$ and as a linear decay for mass smaller than M_c by the same reasoning as before. Meanwhile, for $R_{c2} < R_{c1}$, the mass scales as M^{-3} for R > R_{c1}, as $M^{1/2}$ for $R_{c2} < R < R_{c1}$ and decays linearly for $R < R_{c2}$. Note that the mass function when $R_{c2} > R_{c1}$ is very similar to the previous mass function. In Fig. 8, we show that varying $G\mu$ shifts the peak position and amplitude of the mass for a fixed v^c_{max}. For $R_{c2} > R_{c1}$, initial velocity effects are negligible. However, for $R_{c2} < R_{c1}$ but very close to the value of R_{c1} there is a slight suppression in the region $R_{c2} < R < R_{c1}$ from velocity effects. This is where the importance of v_{max} comes into play. Given a $G\mu$ value, we can run simulations to obtain the associated v_{max}. From plotting it in Fig. 7, we are immediately able to tell the general shape of its accretion distribution.

In Fig. 9, we consider $G\mu = 5.43(10^{-10})$ which minimizes χ^2 in Fig. 6, we find from varying v_{max} that for $v_{max} < 3.00(10^{-2})$, velocity has little effect on mass distribution of globular clusters in the Milky Way galaxy. However, for $v_{max} >> 3.00(10^{-2})$ we will not obtain a mass distribution as the majority of strings will be moving too fast to maintain their accretion.

Analysis 2

In this anlaysis we relax the condition that accretion is exactly spherical using the loop accretion sphericity equation $b(t)$ (described in, (28) such that $b(t) = 1$ for a nearly spherical object and decreases for more elliptical shapes) by consider a slightly lower bound by setting $b(t) > 10^{-1}$. Evaluating for v_i we find that the upper bound on the initial velocity of accreting loops in this analysis differs by only a factor of $10^{1/3}$ from the upper bound found in the first analysis. From here, performing the same steps as in Analysis 1 would obtain results that are larger by a factor $10^{1/3}$. We can understand this as being due to the accretion being stretched in the direction of loop motion; this forces the loop to travel further to disrupt its accretion. This effect can be seen clearly by determining the new v^c_{max} and graphing it as in Fig. 10.

Accretion Retention in Different Geometries

As an interesting aside, we can model highly nonspherical accretions that arise from very fast-moving loops by following the analysis in. (28) First, we determine half of the turnaround mass from a string with some initial velocity approximated by a paraboloid. Assuming that the accreted mass has uniform density, we then approximate the other half of the accreted mass to be spherical. This gives the total mass:

$$M^{ns}_t = (4/5)ma(t). \quad [7]$$

Comparing this to the mass from spherical accretion $M^s_t = (2/5)ma(t)$, we see that non-spherical accretion results in a mass that is larger by a factor of two.

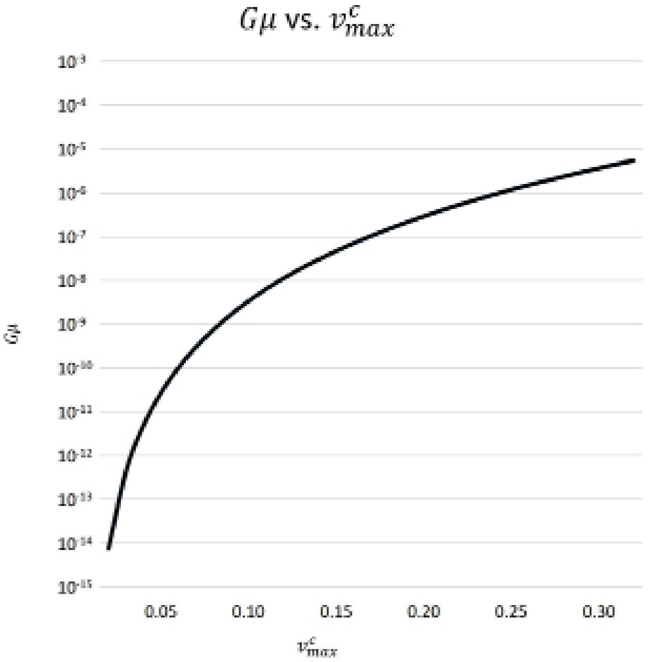

Fig. 10. Analysis 2 - Relation between Gμ and v^c_{max} for $b(t) = 10^{-1}$. The horizontal axis is velocity on a linear scale and the vertical axis gives the Gμ on a logarithmic scale. As before if, for a given Gμ, vmax (as determined by simulations) falls into the region above the curve then $R_{c1} > R_{c2}$; and $R_{c1} < R_{c2}$ if v_{max} is in the region below the curve.

Conclusion & Discussions

The calculations above indicate that the mass distribution of string loops with mass per unit length $G\mu \sim 10^{-9.5}$ accurately explains the origin of globular clusters. In our model, we hypothesize that the string loops that dominate the loop mass distribution at t_{eq} act as seeds for globular cluster formation. Without taking into account velocities (i.e. loops have no initial velocity, v_i), we predict that the number of globular clusters in a galaxy will be proportionate to the mass of the galaxy.

When initial velocity is taken into account, we see that these translational motions play a small but noticeable role in the accretion of matter during the matter-dominated era. We see that cosmic string loops, born in the radiation era with initial velocity v_i, will travel a certain distance. Comparing this distance with the total size of the accreted matter gave rise to two distinct critical radii, R_{c1} and R_{c2}. In another analysis, we demanded that $b(t) > 10^{-1}$. This ensures that the accreted object is roughly spherical in shape. Our theory predicts a cutoff velocity: any loops with higher translational speeds will simply not form any observable objects.

Aside from globular clusters, it is noteworthy to mention that the analyses discussed in this report may also be applied to ultra-compact-mini-halos, as they too can be manifestations of cosmic string loop accretions. One question not discussed here is the formation of stars inside the accreted matter. (29, 30) It is entirely possible that there will be a significantly different star formation process for matter accreting onto a string loop inside a galaxy, as opposed to in a field (open area) in between galaxies.

Acknowledgements

We wish to thank R. Brandenberger for useful discussions and encouragement

References

1. Centre for Theoretical Cosmology, “The Origins of the Universe: Cosmic defects,” Web. Aug. 2016.
2. R. Nemiro and J. Bonnell, “Astronomy Picture of the Day,” Web. Aug. 2016.
3. W. E. Harris, “Massive star clusters in galaxies,” Philosophical Transactions of the Royal Society of London Series A, vol. 368, pp. 889–906, Jan. 2010.
4. J. P. Brodie and J. Strader, “Extragalactic Globular Clusters and Galaxy Formation,” ARA&A, vol. 44, pp. 193–267, Sept. 2006.
5. R. Battye and A. Moss, “Updated Constraints on the Cosmic String Tension,” Phys. Rev. D, vol. 82, p. 023521, 2010. [arXiv:1005.0479].
6. P. D. Mauskopf and et al. [Boomerang Collaboration], “Measurement of a Peak in the Cosmic Microwave Background Power Spectrum from the North American test flight of BOOMERANG,” Astrophys. J, vol. 536, p. L59, 2000. [arXiv:astro-ph/9911444].
7. A. K. [the ACT Collaboration], “The Atacama Cosmology Telescope Project: A Progress Report,” NewAstron. Rev, vol. 50, p. 969, 2006. [arXiv:astro-ph/0608549].
8. J. L. Sievers and et al. [Atacama Cosmology Telescope Collaboration], “The Atacama Cosmology Telescope: Cosmological parameters from three seasons of data,” JCAP, vol. 1310, p. 060, 2013. [arXiv:1301.0824].
9. J. E. Ruhl and et al. [The SPT Collaboration], “The South Pole Telescope,” Proc. SPIE Int. Soc. Opt. Eng., vol. 5498, p. 11, 2004. [arXiv:astro-ph/0411122].
10. Z. Hou, C. L. Reichardt, K. T. Story, B. Follin, R. Keisler, K. A. Aird, B. A. Benson, L. E. Bleem, and et al., “Constraints on Cosmology from the Cosmic Microwave Background Power Spectrum of the 2500 deg 2 SPT-SZ Survey,” Astrophys. J., vol. 782 no. 2, p. 74, 2014. [arXiv:1212.6267].
11. C. L. Bennett and et al., “First Year Wilkinson Microwave Anisotropy Probe

(WMAP) Observations: Preliminary Maps and Basic Results," Astrophys. J. Suppl., vol. 148, p. 1, 2003. [arXiv:astro-ph/0302207].
12. P. A. R. Ade and et al. [Planck Collaboration], "Planck 2013 results. XVI. Cosmological parameters," Astron. Astrophys, vol. 571, p. A16, 2014. [arXiv:1303.5076].
13. C. Dvorkin, M. Wyman, and W. Hu, "Cosmic String constraints from WMAP and the South Pole Telescope," Phys. Rev. D, vol. 84, p. 123519, 2011. [arXiv:1109.4947].
14. P. A. R. Ade and et al. [Planck Collaboration], "Planck 2013 results. XXV. Searches for cosmic strings and other topological defects," Astron. Astrophys., vol. 571, p. A25, 2014. [arXiv:1303.5085].
15. R. J. Danos and R. H. Brandenberger, "Canny Algorithm, Cosmic Strings and the Cosmic Microwave Background," Int. J. Mod. Phys. D, vol. 19, p. 183, 2010. [arXiv:0811.2004].
16. S. Amsel, J. Berger, and R. H. Brandenberger, "Detecting Cosmic Strings in the CMB with the Canny Algorithm," JCAP, vol. 0804, p. 015, 2008. [arXiv:0709.0982].
17. A. Stewart and R. Brandenberger, "Edge Detection, Cosmic Strings and the South Pole Telescope," JCAP, vol. 0902, p. 009, 2009. [arXiv:0809.0865].
18. R. Battye and A. Moss, "Updated constraints on the cosmic string tension," Phys. Rev. D, vol. 82, p. 023521, 2010. [arXiv:1005.0479].
19. A. Vilenkin, "Cosmic Strings," Phys. Rev. D, vol. 24, p. 2082, 1981.
20. T. W. B. Kibble, "Evolution of a System of Cosmic Strings," Nucl. Phys. B, vol. 252, p. 227, 1985.
21. T. Vachaspati and A. Vilenkin, "Gravitational Radiation from Cosmic Strings," Phys. Rev. D, vol. 31, p. 3052, 1985.
22. A. Barton, R. H. Brandenberger, and L. Lin, "Cosmic strings and the origin of globular clusters," JCAP, vol. 06, 2015.
23. R. H. Brandenberger, "Topological Defects and Structure Formation," Int. J. Mod. Phys. A9, p. 93, 1994. [arXiv:astro-ph/9310041].
24. Y. B. Zel'dovich, "Gravitational Instability: An Approximate Theory for Large Density Perturbations," A&A, vol. 5, p. 84, 1970.
25. O. Y. Gnedin and J. P. Ostriker, "Destruction of the Galactic Globular Cluster System," ApJ, vol. 474, p. 223, 1997. [arXiv:astro-ph/9603042].
26. J. J. Blanco-Pillado, K. D. Olum, and B. Shlaer, "Large Parallel Cosmic String Simulations: New Results on Loop Production," Phys. Rev. D, vol. 83, p. 083514, 2011. [arXiv:1101.5173].
27. M. Pagano and R. H. Brandenberger, "The 21cm Signature of a Cosmic String Loop," JCAP, vol. 05, p. 014, 2012. [arXiv:1201.5695].
28. E. Bertschinger, "Cosmological Accretion Wakes," ApJ, vol. 316, p. 489, 1987.
29. B. Shlaer, A. Vilenkin, and A. Loeb, "Early Structure Formation from Cosmic String Loops," JCAP, vol. 05, p. 026, 2012. [arXiv:1202.1346].
30. F. Duplessis and R. Brandenberger, "Note on Structure Formation from Cosmic String Wakes," JCAP, vol. 1304, p. 045, 2013. [arXiv:1302.3467].